# Investigation of the fracture behavior of tungsten at the micro scale

Nicola J. Schmitt[1,*], Christoph Bohnert[1,2], Christoph Eberl[1,3], Ruth Schwaiger[1], Sabine M. Weygand[2], Oliver Kraft[1]

[1)] Institute for Applied Materials (IAM), Karlsruhe Institute of Technology (KIT), Hermann-von-Helmholtz-Platz 1, 76344 Eggenstein-Leopoldshafen (Germany)

[2)] Faculty of Mechanical Engineering and Mechatronics (MMT), Karlsruhe University of Applied Sciences, Moltkestr. 30, 76133 Karlsruhe (Germany)

[3)] Fraunhofer Institute for Mechanics of Materials (IWM), Wöhlerstraße 11, 79108 Freiburg (Germany)

*Corresponding author: nicola.schmitt@kit.edu

**Abstract** Tungsten promises great potential in very high temperature applications due to its very high melting point. Yet its brittleness, far above room temperature, limits its application. Investigations have already shown that fracture toughness of polycrystalline tungsten strongly depends on microstructural characteristics like grain size and shape, and texture. To gain a better insight into the basic mechanisms, fracture toughness experiments are carried out at the micro-scale. First experiments focus on the influence of the crystal orientation with respect to cracking. Here, we report on micro bending tests on free standing, notched, single crystal micro cantilevers. With respect to the {110}<$1\bar{1}0$> crack system, the beam axis was normal to the {110} crystal plane.

**Keywords** Tungsten, fracture toughness, crystal orientation, micro bending experiments

## 1. Introduction

Tungsten is a very promising material for power generation due to its outstanding properties at high temperatures such as high strength, high Young's modulus, and of course its high melting point. A huge drawback, though, is its brittleness and high brittle-to-ductile temperature which limits the use of tungsten significantly. Therefore, several studies have already been carried out to investigate the fracture behavior and to provide suitable remedies.

An extensive study of the fracture toughness of tungsten single crystals had been carried out by Riedle and Gumbsch [1-3]. They considered the influence of crystal orientation, loading rate, and temperature on the fracture behavior. Furthermore, studies on the fracture behavior of polycrystalline tungsten were reported by Gludovatz et al. [4], who investigated pure polycrystalline tungsten as well as doped tungsten to gain different microstructures at various temperatures. Experiments on pure rolled polycrystalline tungsten were carried out by Rupp and Weygand [5]. They observed the influence of different grain boundary orientations on the fracture behavior. All those investigations showed that fracture toughness in single crystal and commercial polycrystalline tungsten strongly depend on microstructural characteristics and loading conditions. However, most studies were carried out at the macro-scale with few exceptions such as Wurster et al. [6] who studied the fracture behavior of single crystalline tungsten at the micro-scale.

The aim of this study is to observe the fracture behavior of tungsten at the micro-scale to deepen the insight into the fracture behavior of tungsten on a micromechanical basis. For this, free standing single crystal bending cantilevers with a typical dimension of 20 µm in width and 40 µm in height have been manufactured and tested using a nanoindenter. To investigate the influence of different crack systems, experiments will be carried out with differently oriented beams. Further experiments on bi-crystals will be conducted in situ using the SEM to see the influence of grain boundary. Here, we report on the development of the testing procedure as well as first results for beams that are oriented to induce fracture in the {110}<1$\bar{1}$0> crack system. The investigations are accompanied by crystal plasticity simulations [7] addressing the interplay of cracking and plastic deformation at small scale.

## 2. Experimental

Tungsten single crystals with 3 mm in width and height and 5 mm in length were used for the manufacturing of the free-standing micro bending beams. The samples were aligned in a specific crystal orientation.
At the scale the experiments are conducted, the standard geometry and procedure of the ASTM E 399-90 for the determination of the fracture toughness does not apply, the plastic zone is too large relative to the cantilever dimensions. Also, no standardized testing device is available to conduct standard fracture toughness tests at this length-scale. Therefore, a new specimen geometry was developed which is shown in Figure 1. The geometry is a result of the available manufacturing and testing conditions. To design the experiment close to the standard test, the relations of width, length, and height are derived from the ASTM E 399-90 for standard fracture toughness tests. As the samples are going to be tested with a nanoindenter free-standing cantilevers were chosen. The length of the cantilevers is roughly 160 µm, the width is 33 µm and the height is 40 µm. At this scale the focused ion beam (FIB, FEI Company, Nova 200 NanoLab) is an accurate and nearly inevitable tool, yet at the targeted dimensions it is rather time consuming and inefficient. Therefore, the basic cantilevers were carved by a micro electrical discharge machining (µ-EDM) process. The actual width of the gage section width is thinned to 20 µm and the notch is cut to a depth of 20 µm at a distance of 50 µm from the shoulder using a focused ion beam (FIB). The radii between the bulk material and the cantilever are roughly 20 µm which can be realized reliably by µ-EDM. Due to the manufacturing process, however, the geometry varies from the design dimensions, and the size and shape of each individual beam is inspected by scanning electron microscopy (SEM).

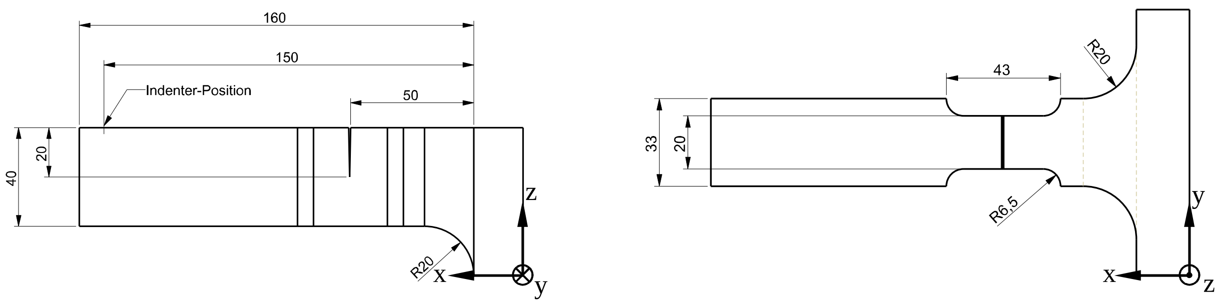


Figure 1. Developed free standing micro bending beam geometry as a result of manufacturing and testing restrictions.

In the first preparation step, the samples were mechanically polished using a Struers TriPod polishing fixture and Allied diamond lapping foils (9 µm, 6 µm, 3 µm, 1 µm, 0.5 µm). This results in an almost plane surface and sharp edges. This is necessary, as the bending cantilevers will be carved from the edges of the single crystals. Rounded edges would lead to cantilevers with decreasing thickness.

A custom-built specimen holder based on a goniometer was used to align the samples accurately for the µ-EDM process. First, a thin plate with the thickness of the cantilevers was prepared by a horizontal cut parallel to the polished surface. Afterwards, every single cantilever was carved from the thin plate by vertical cuts.

Due to the heat input and the re-deposition of molten material, the µ-EDM process results in a rather rough surface of the micro cantilevers. Also micro-cracks and changes of the microstructure may be possible. The µ-EDM exposed surfaces did not yield a diffraction pattern when investigated by electron backscatter diffraction (EBSD). However, EBSD investigations on a beam cross-section after EDM showed that less than 1 µm beneath that modified layer the EBSD pattern indicates no orientation changes, with respect to the initial material. Thus, we conclude that the beams remain single crystalline after the EDM process.

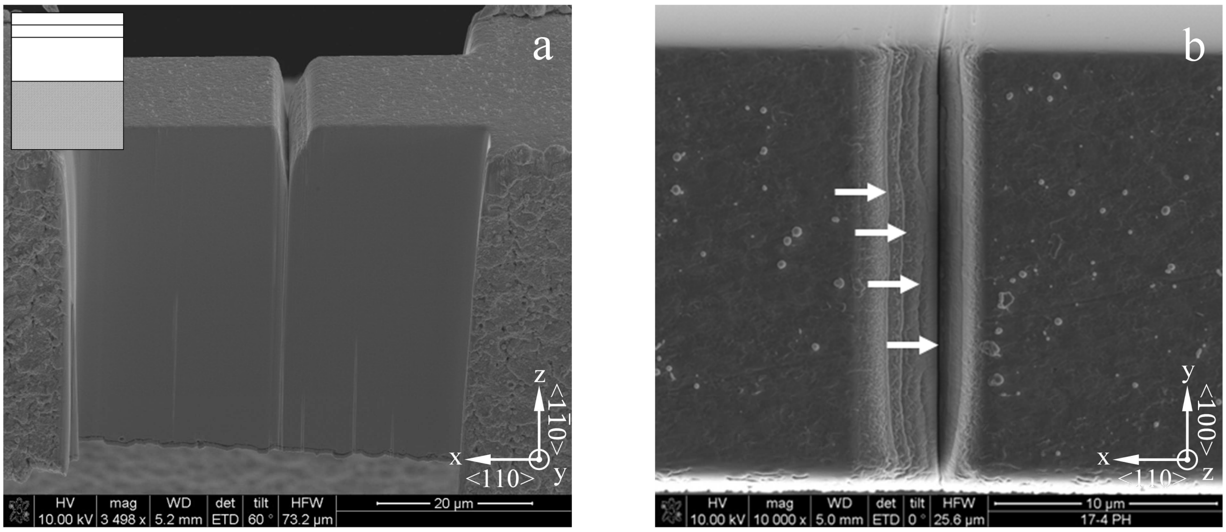


Figure 2. SEM micrographs showing the introduced notch which is cut with the ion beam perpendicular to the surface. The SEM micrograph 2a shows the cleaned gage section and the notch from the side. The insert shows a schematic cross-section of the notch. The SEM micrograph 2b shows a top-view. The arrows show the individual millings steps for 5, 3, 1 µm and the line milling mode.

To minimize the influence of µ-EDM processing, FIB was used to polish the gage sections of the cantilevers. Successive cutting from the surface towards the middle of the beam by FIB was conducted to remove the damage layer, to machine the necessary dimensions, and to smoothen the surface of the beam. For all milling steps an acceleration voltage of 30 kV was used. To remove the main part of the material relatively high gallium ion currents of 5 to 20 nA were applied. In order to reduce the influence of the gallium ions in the material the last cleaning steps were carried out by lower gallium ion currents of 1 to 3 nA. Finally, a notch was cut from the top surface with a depth of approximately 8 µm. For the notches a current of 1 nA was used. In order to gain a deep and sharp notch the machining process was carried out in several milling steps. The steps were successively narrowed from 5 to 3 and 1 µm and as a last milling step, the final notch was introduced using the line milling mode. The ion beam was always perpendicular to the surface. Figure 2 shows the notch shape.

The successive milling process of the gage section showed that the µ-EDM induced micro-cracks. However, they never reached deeper than 3 µm. Therefore, the milling process was adjusted such that roughly 4 µm of the material was removed to exclude the influence of micro-cracking on the fracture behavior. Figure 3 shows a typical surface of a micro-cantilever which was treated by µ-EDM, micro-cracks can be observed.

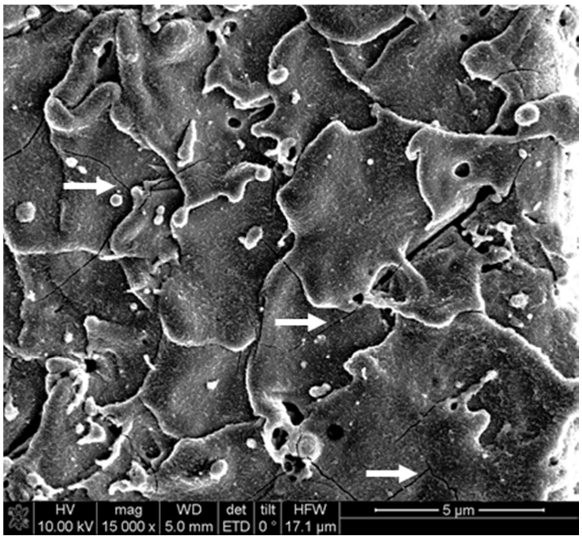


Figure 3. The rough surface of the micro cantilever as a result of the µ-EDM process. Micro cracks in the surface can be observed. The white arrows highlight some of the micro cracks.

For the bending experiments two commercially available nanoindentation systems were used (MTS, Nano Indenter XP and Agilent Technologies, G200). The indenter tip was used to bend the cantilever at a defined distance to the notch. Then, a holding segment of 10 seconds was applied before unloading. For all experiments a Berkovich tip was used. Afterwards the broken cantilevers were investigated by scanning electron microscopy (SEM).

## 3. Results and Discussion

The force-displacement curves shown in Figure 4 belong to two beams that are oriented to induce fracture in the {110}$<1\bar{1}0>$ crack system. The cantilevers were displaced to 12 µm (blue curve) and 15 µm (green curve) at a distance of about 120 µm from the notch. As the maximum displacement is reached, the holding segment follows and the maximum load is held constant. The curve shows clearly an elastic-plastic transition but no abrupt load drop which would be indicative of brittle fracture. Interestingly, a large deflection takes place during the hold segment. Presumably this is caused by an increasing crack length over time which in turn is correlated to an increasing $\Delta K$ under constant load. Since this is a rather peculiar behavior, it will be investigated further by changing the loading sequence of the test.

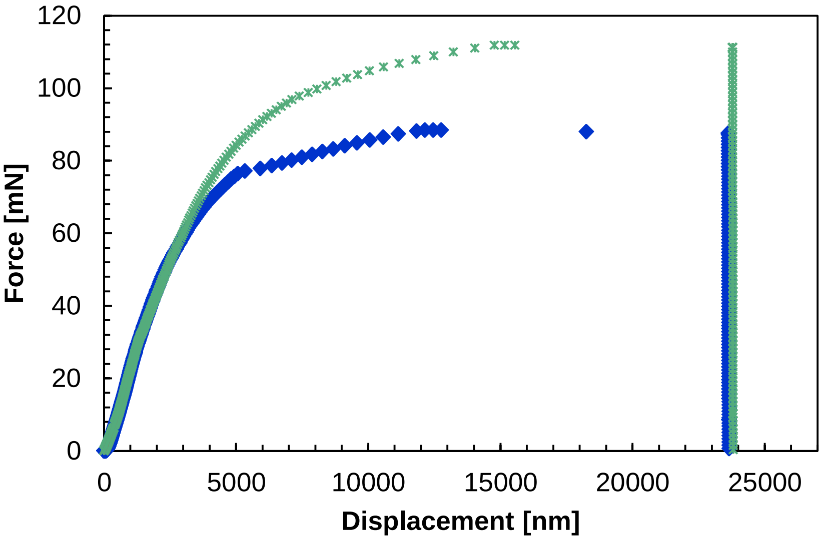


Figure 4. Two force-displacement curves of two notched beams. One beam was loaded to a displacement of 12 μm (blue curve) the other one to 15 μm (green curve) (Figure 5a). With respect to the {110}<1$\bar{1}$0> crack system, the beam axis was normal to the {110} crystal plane for both notched beams.

The curves show a rather ductile behavior, however, an investigation of the fractured surface indicates partially brittle failure. Figure 5a shows the fractured beams and Figure 5b and c the surface of the broken cantilevers. It clearly shows brittle cleavage in the middle of the beam, while at the upper edges signs of plastic deformation are seen.

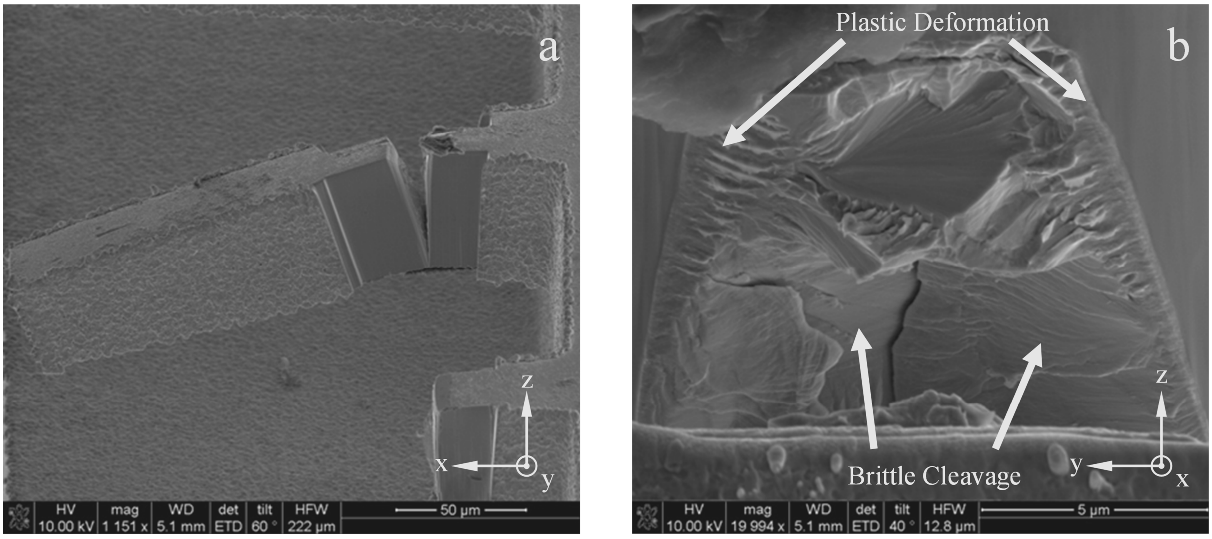

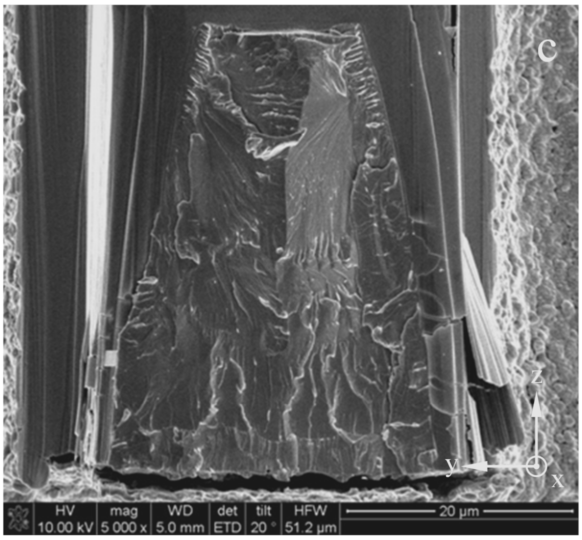


Figure 5. a) Post-test overview of beam 1 and 2. b) Cleavage surface of beam 1 which was deflected 12 µm under displacement control and fractured further under constant load. The beam did not fail completely. c) Cleavage surface of beam 2 which was displaced 15 µm. It fractured completely during the holding segment

The fracture toughness cannot be calculated following the ASTM E 399-90 as it does not apply at this small scale. Also, it is not trivial to determine the weight function for this geometry. Therefore, we take a simplistic approach to estimate the fracture toughness by looking at an energy relation. Equation (1) relates the fracture toughness $K_Q$ and the energy release rate $G_Q$ were E is Young's modulus [8].

$$K_Q^2 = G_Q \cdot E, \quad (1)$$

Thereby $G_Q$ can be calculated after [9]:

$$G_Q = \frac{d(W - U_{el})}{dA}, \quad (2)$$

Here, W is the work of the external forces, $U_{el}$ the elastically stored energy and d$A$ the change of the area of the crack which is taken here to be the entire fracture plane. As the elastically stored energy $U_{el}$ is subtracted from the external forces $W$, the shape modification energy only remains. To gain the work of the external forces, the load-displacement curve was integrated. For the elastically stored energy, the area enclosed by Hook's' straight line and the curve at the maximum displacement was calculated. For the calculation of the size of the fracture plane the program ImageJ was used. Therefore, the fracture surface, depicted in an SEM Image, was enclosed by a polygon. The resulting surface area was calculated by the program in dependence of the SEM magnification. With this calculation, values of the fracture toughness $K_Q = 31$ MPa·m$^{1/2}$ and 35 MPa·m$^{1/2}$ were obtained when including the displacement during the hold segment. These values are quite high and can be only considered as an upper bound. For a lower bound, a second value was calculated neglecting the holding segment. Thereby, values for the fracture toughness $K_Q$ of 6.7 MPa·m$^{1/2}$ and 5.9 MPa·m$^{1/2}$

were obtained. These values are pretty low compared to data of Gumbsch and Riedel [1,3] of $12.9 \pm 2.1$ MPa·m$^{1/2}$ for the fracture toughness of the {110}<1$\bar{1}$0> crack system. However, the experiments are not completely comparable as different sample dimensions and loading conditions were used. As shown in Figure 5, for our small samples, it is seen that the plastic zone size is large relative to the sample dimensions. Therefore, we would rather expect a larger value than the one reported by Riedel and Gumbsch. This also confirms the need to improve the test method. Errors in the fracture surface analysis cannot account for the large difference.

Improvements in the manufacturing process, testing conditions and also analysis are currently in progress. For instance, the surface of the basic material can be treated by µ-EDM. This would lead to sharper edges. Therefore, cantilevers with decreasing cross sections along the axis will be avoided, compared to the polishing with the Struers TriPod and diamond lapping foils. Also, a wedge tip will be used instead of the Berkovich tip in order to avoid slipping and other effects related to the point loading.

Most importantly, another notch geometry will be tested. As it is not possible to introduce a sharp crack via fatigue at this specimen dimension, a Chevron notch geometry will be tested in the future. This should lead to a more controlled crack propagation as the resistance against crack propagation will increase with increasing crack propagation. An example of the FIB machined Chevron notch geometry is shown in Figure 6. For fabrication, the specimen was tilted so that the ion beam cut the specimen at an angle of about 30°. The middle of the width of the specimen, where the notch should be placed, was marked by FIB. From this mark, the notch was cut under the given angle, then the specimen was rotated by 180° and the second part of the notch was milled.

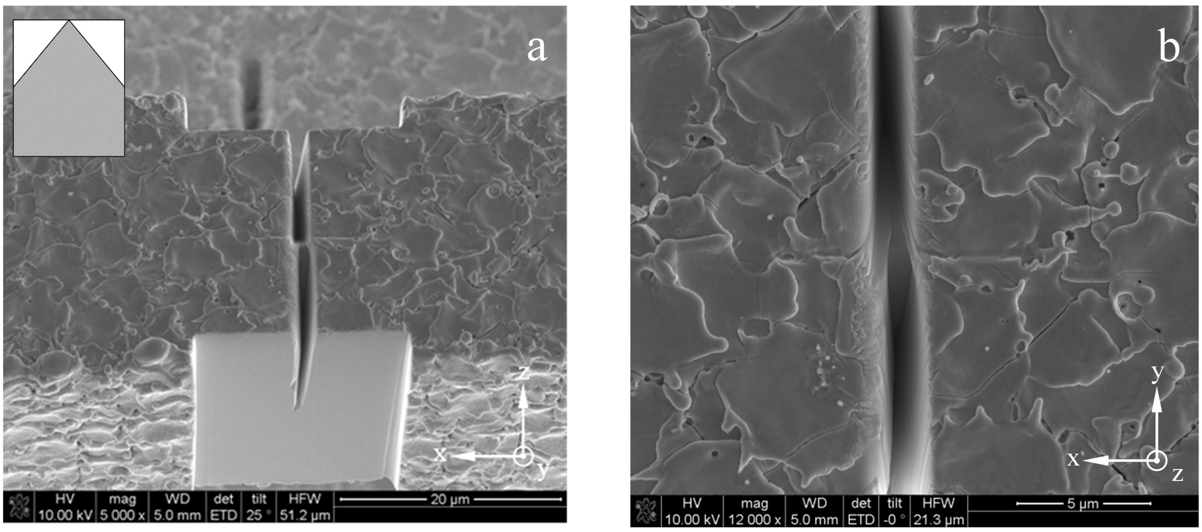


Figure 6. The introduced Chevron notch. The SEM micrograph 6a shows the cleaned gage section and the notch from the side. The insert shows a schematic cross-section of the Chevron notch. The SEM micrograph 6b shows the top-view.

## 4. Summary

The fracture toughness of single crystalline tungsten for the $\{110\}\langle 1\bar{1}0\rangle$ crack system at the micro scale has been investigated. Free-standing single crystal micro cantilevers were manufactured by μ-EDM followed by surface cleaning and cutting a notch by FIB. The micro cantilevers were tested with a nanoindenter. The cantilever axes were aligned with the normal direction of the {110} crystal plane, while the loading direction was parallel to the $\langle 1\bar{1}0\rangle$ direction. The force-displacement curves show a rather elastic-plastic behavior, whereas the observation of the fracture surface reveals ductile features at the edges of the crack surface and brittle ones in the middle. The $K_Q$ values were estimated via an energy relation. The estimated values were in a range between 5.9 and 35 $MPa\cdot m^{1/2}$ as the lower and upper limits. Further improvements of the test method will be made in the future including optimizing the beam shape, testing method as well as the notch shape. Furthermore, the investigations will be extended towards other crack systems as well as bi-crystals and in situ experiments in the SEM.

**Acknowledgements**

The authors thank Christoph Ruhs and the Institute of Production Science of the Karlsruher Institute of Technology for the implementation of the μ-EDM process.
Also, thank goes to the Landesgraduiertenförderung of the state of Baden-Württemberg in the framework of the Promotionskolleg on ”Gefügestrukturanalyse und Prozessbewertung” for their financial support.

**References**

[1] P. Gumbsch, Brittle fracture and the brittle-to-ductile transition of tungsten. J Nucl Mater 2003; 323:304-12.
[2] J. Riedel, Bruchwiderstand in Wolfram-Einkristallen: Einfluss der kristallographischen Orientierung, der Temperatur und der Lastrate. Reihe 18 – Nr. 184: Düsseldorf: VDI Verlag; 1990.
[3] J. Riedel, P. Gumbsch, H. Fischmeister, Cleavage anisotroy in tungsten single crystals. Phys Rev Lett 1996;76:3594-7
[4] B. Gludovatz, S. Wurster, A. Hoffmann, R. Pippan, Fracture toughness of polycrystalline tungsten alloys. Int J of Refrac Met and Hard Mat 2010;28:674-678
[5] D. Rupp, S. M. Weygand, Experimental investigation of the fracture toughness of polycrystalline tungsten in the brittle and semi-brittle regime. J Nucl Mater 2009;386-388:591-593
[6] S. Wurster, C. Motz, R. Pippan, Characterization of the fracture toughness of micro-sized tungsten single crystal notched specimens. Philos Mag 2012;92:1803-1825
[7] C. Bohnert, S. M. Weygand, N. J. Schmitt, O. Kraft, Numerical Investigation of the Fracture Behavior of Tungsten at the Micro scale, ICF13th International Conf. on Frature, Beijing, 2013
[8] J. Rösler, H. Harders, M. Bäker, Mechanisches Verhalten der Werkstoffe. B. G. Teubner Verlag/GWV Fachverlage GmbH, Wiesbaden 2003
[9] H. Blumenaue, G. Pusch, Technische Bruchmechanik, WILEY-VCH Verlag GmbH & Co. KgaA, Weinheim 2001